ORIGINAL ARTICLE

Gray and White Matter Brain Abnormalities in First-Episode Schizophrenia Inferred From Magnetization Transfer Imaging

Manny S. Bagary, MRCPsych; Mark R. Symms, PhD; Gareth J. Barker, PhD; Stan H. Mutsatsa, MSc; Eileen M. Joyce, PhD, FRCPsych; Maria A. Ron, FRCPsych

Background: Neuroimaging studies suggest that schizophrenia is associated with gray and possibly white matter changes. It is unclear whether these changes are present at illness onset or which brain structures are selectively affected. New imaging methods such as magnetization transfer imaging may be more sensitive than conventional volumetric imaging to the subtle structural brain changes in schizophrenia.

Methods: High-resolution volumetric T1-weighted images and magnetization transfer images were acquired from 30 patients (29 with first-episode schizophrenia and 1 with schizophreniform psychoses) and 30 control subjects. Images were processed using voxel-based morphometry, which allows whole-brain analysis.

Results: Compared with controls, the magnetization transfer ratio (an index of signal loss derived from magnetization transfer imaging) was reduced bilaterally in the medial prefrontal cortex (right greater than left), insula (left greater than right), and white matter incorporating the fasciculus uncinatus (left greater than right) in the patient group. Analysis of the T1-weighted images did not reveal significant volumetric differences between patients and controls.

Conclusions: Gray and white matter abnormalities are present in schizophrenia at illness onset. The magnetization transfer ratio is sensitive to these abnormalities, which cannot be explained by detectable atrophy in our patient group.

Arch Gen Psychiatry. 2003;60:779-788

From the Department of Neuroinflammation, Institute of Neurology, Queen Square, University College London (Drs Bagary, Symms, Barker, and Ron), and Division of Neuroscience and Psychological Medicine, Imperial College Faculty of Medicine, Charing Cross Campus (Mr Mutsatsa and Dr Joyce), London, England.

A RECENT REVIEW[1] concluded that magnetic resonance imaging (MRI) brain abnormalities are common in schizophrenia populations. Frequencies of regional changes, expressed as a percentage of studies reviewed, were 100% for volume loss in the superior temporal gyrus, 74% for medial temporal structures, 59% for prefrontal regions, 31% for the cerebellum, and 80% for ventricular enlargement.[1] A contemporary meta-analysis[2] also reported increased ventricular volume and decreases in medial temporal lobe structures and cerebral volume. Converging evidence from neuroimaging, neuropathological, and neurocognitive studies suggests that abnormalities in frontotemporal, frontostriatal,[3-7] and frontothalamic-cerebellar[8] pathways may explain many of the clinical manifestations of schizophrenia. It remains uncertain whether structural changes are reversible[9] or progressive, at least in some patients,[10] and whether different clinical and cognitive phenotypes are associated with distinctive brain abnormalities.

Recently, attention has focused on first-episode schizophrenia, in which detectable brain abnormalities are more likely to reflect the primary disease process, diminishing confounds such as medication exposure and chronicity. In their review, Shenton et al[1] concluded that abnormalities described in patients with first-episode schizophrenia were similar to those in chronic schizophrenia populations. Reduced gray matter volume,[11,12] increased ventricular volumes,[13,14] and temporolimbic abnormalities[15,16] are the most commonly reported abnormalities in first-episode schizophrenia. Hippocampus volume reduction has been considered one of the most consistent structural abnormalities in schizophrenia, and it may be present at illness onset.[17] Perhaps because early structural changes may be subtle and patients with first-episode schizophrenia are more likely to have variable disease outcomes, some such studies have not found significant volumetric abnormalities for ventricles and temporal lobes,[18] regional or total hemisphere volumes,[19] and the hippocampus or parahippocampal gyrus.[20,21] Although high-resolution imaging continues to improve sensitivity with progressively decreasing slice thickness, the limitations of volu-

Table 1. Demographic and Clinical Data for 60 Study Participants

Variable	Patients With First-Episode Schizophrenia (n = 30)*	Control Subjects (n = 30)
Sex, M/F, No.	19/11	18/12
Age, mean ± SD (range), y	27.3 ± 7.4 (18-47)	28.9 ± 5.5 (21-49)
Handedness, left/right, No.	3/27	2/28
Paternal social class, rank-order range	1-34	1-33
NART premorbid IQ, mean ± SD	110 ± 8.4	113 ± 6.4
Illness duration at time of scan, mean ± SD (range), mo†	5.33 ± 4.3 (1-14)	NA
Medications, typical/atypical/nil, No.	6/19/5	NA
SAPS score, mean ± SD	12.63 ± 4.4	NA
SANS score mean ± SD	11.9 ± 6.6	NA
CPRS score, mean ± SD	57.5 ± 20.2	NA

Abbreviations: CPRS, Comprehensive Psychopathological Rating Scale[41]; NA, not applicable; *NART*, National Adult Reading Test[44]; SANS, Scale for the Assessment of Negative Symptoms[40]; SAPS, Scale for the Assessment of Positive Symptoms.[40]

*Twenty-nine patients with schizophrenia and 1 with schizophreniform psychosis.

†Number of months since first receiving psychiatric services.

metric MRI include lack of neuropathological specificity and poor sensitivity to subtle neuropathological changes that may not culminate in atrophy. In schizophrenia neuroimaging, the enhanced sensitivity and neuropathological specificity of magnetization transfer imaging (MTI) offers considerable advantages.

First described by Wolff and Balaban,[22] MTI is based on the interaction of protons bound to macromolecular structures and free protons in tissue water. In brain tissue, the major macromolecules in the bound proton pool are thought to be cell membrane proteins and phospholipids in gray matter and myelin in white matter. Bound protons are preferentially saturated using an off-resonance radiofrequency pulse. Chemical exchange or direct dipolar coupling transfers macromolecular saturation from bound to free protons, causing decreased longitudinal magnetization undetected by conventional MRI because bound protons have short relaxation times in biological tissues. The reduction in signal intensity depends on macromolecular density. The nature of the interaction sites has yet to be fully determined.[23] However, creatine-containing compounds seem to be involved in through-space dipolar interactions to a greater extent than glutamine/glutamate, *N*-acetylaspartate, and lactate, whereas chemical interaction may be more important for the latter.[24] The degree of signal loss, measured in percentage units, is the magnetization transfer ratio (MTR).

An MTR reduction correlates with myelin and axonal loss in postmortem tissue from the spinal cord[25] and brain[26] in multiple sclerosis, experimental allergic encephalitis,[27] toxic demyelination,[28] wallerian degeneration,[29] and experimental brain injury.[30] In vivo white matter MTR decreases occur in conditions with myelin or axonal loss, for example, multiple sclerosis,[31] central pontine myelinolysis,[32] cerebral ischemia,[33] systemic lupus,[34] human immunodeficiency virus infection,[35] and traumatic brain injury.[36] Gray matter abnormalities have been studied less extensively, but wallerian degeneration triggered by distant axonal damage and microscopic lesions are thought to explain cortical MTR reductions in multiple sclerosis.[37] The first study to use MTI in chronic schizophrenia[38] reported widespread cortical MTR reductions indicative of subtle structural abnormalities, which may reflect reported changes in dendritic density.[39]

To the best of our knowledge, this study is the first application of MTI to the investigation of patients with first-episode schizophrenia, whom we compared with healthy volunteers using the MTR, an index of signal loss derived from MTIs. We also acquired high-resolution volumetric images to assess for atrophy. Voxel-based morphometric (VBM) analysis was used to study group differences using both types of imaging because VBM reduces observer bias and allows whole-brain analysis. Our hypothesis was that frontotemporal abnormalities would be detectable by the time patients first present to medical attention. Based on findings in chronic schizophrenia,[38] we further predicted that the MTR would be more sensitive to these abnormalities than conventional T1-weighted volumetric imaging.

METHODS

PARTICIPANTS

Thirty patients (19 were men and 3 were left-handed) with a mean age of 27.3 years (range, 18-47 years) were examined. The catchment area included deprived inner city and affluent suburban areas of London. Patients were recruited as soon as possible after first presenting to mental health services with schizophreniform psychosis (*DSM-IV*). Diagnostic criteria were reviewed by 2 experienced clinicians (E.M.J.) 1 year after recruitment to establish a diagnosis of schizophrenia. One patient was lost to follow-up before this diagnostic review. Antipsychotic medications included olanzapine, risperidone, sulpiride, haloperidol, and zuclopenthixol (19 patients used atypical agents, 6 used typical agents, and 5 were unmedicated). Symptom severity was assessed using the Scale for the Assessment of Negative Symptoms, the Scale for the Assessment of Positive Symptoms,[40] and the Comprehensive Psychopathological Rating Scale.[41] We also determined handedness[42] and parental social class[43] and estimated premorbid IQ using the *National Adult Reading Test*.[44] **Table 1** summarizes demographic and clinical indices.

Thirty healthy volunteers (18 were men and 2 were left-handed) with a mean age of 28.9 years (range, 21-49 years) were recruited to match the patient group for age, sex, handedness, and estimated premorbid IQ. Controls with a history of neurological or systemic illness, head injury, substance abuse, or alcohol intake greater than 240 g/wk were excluded. Controls with a personal or family history of psychiatric illness were also excluded. Permission to conduct the study was obtained from all relevant research ethics committees. Written informed consent was obtained from all participants. A neuroradiologist reviewed the brain MRIs. No gross abnormalities were reported.

MAGNETIC RESONANCE IMAGING

Participants underwent MRI using a 1.5-tesla scanner (Signa; GE Medical Systems, Waukesha, Wis) with a standard quad-

rature head coil. Total scanning time (including sequences not reported herein) was 60 minutes. A preliminary sagittal localizing scan was acquired. High-resolution coronal volumetric images were acquired using a 3-dimensional T1-weighted spoiled gradient recalled echo (SPGR) sequence generating 124 contiguous, 1.5-mm coronal slices (echo time, 4.2 milliseconds; repetition time, 15 milliseconds; field of view, 24 cm^2; 256×192 matrix; and flip angle, 20°). The 1.0×1.2×1.5-mm acquisition parameters were determined by scan time constraints and were automatically reconstructed by the scanner to a 1.0×1.0×1.5-mm voxel size. Axial MTIs were acquired using a dual spin-echo–based MTI sequence (echo time, 30/80 milliseconds; repetition time, 1720 milliseconds; 28 contiguous 5-mm axial slices; 256×128 pixel image matrix; and field of view, 24 cm^2) with and without a saturation pulse (16 milliseconds, 23.2-μT Hamming appodised 3 lobe sinc pulse applied 1 kHz from water resonance). The 1×2×5-mm MTI acquisition parameters were determined by scan time constraints. The scanner automatically reconstructed images to a 1×1×5-mm voxel size. The MTI sequence described in detail by Barker et al[45] generates proton-density and T2-weighted images along with MT-weighted images. These images are all inherently registered to each other and to the calculated MTR image created from proton-density and MT-weighted images. The MTR is an index of signal loss in percentage units, calculated on a pixel-by-pixel basis from the following formula:

$$MTR = [(M_o - M_s)/M_o] \times 100,$$

where M_s and M_o are mean signal intensities with and without the saturation pulse, respectively. The MTR is not calculated in voxels if values in source images are below the mean background noise level. We used the 30-millisecond echo for MTR calculation because the resulting map has a higher signal-to-noise ratio than that from the 80-millisecond echo. Typical MTR values are 30% to 50% for white matter, 20% to 40% for gray matter, and approaching 0% for cerebrospinal fluid. For our sequence, MTR values were approximately 40% for white matter, 35% for subcortical gray matter, 32% for cortical gray matter, and 2% for cerebrospinal fluid.

IMAGE PROCESSING

Data were processed on a computer workstation (Sun Ultra; Sun Microsystems Inc, Santa Clara, Calif) using SPM99 statistical parametric mapping software (Wellcome Department of Cognitive Neurology, London) and working in an analysis environment (MATLAB; The MathWorks Inc, Natick, Mass), unless otherwise stated.

SPOILED GRADIENT RECALLED ECHO

Images were reoriented into axial slices aligned parallel to the anteroposterior commissural axis. The origin was set to the anterior commissure. Images were spatially normalized to the standard T1 template in SPM99, following a method that optimizes segmentation accuracy for VBM described by Good et al.[46] Affine registration (12 nonlinear iterations, medium nonlinear regularization, resliced to 2×2×2-mm voxels) produced isotropic voxels of higher signal-to-noise ratio than the original images. The images were flipped to neurological space and then segmented using image intensity nonuniformity correction. A mixture model cluster analysis identifies voxel intensities matching tissue types (gray matter, white matter, and cerebrospinal fluid) combined with a priori knowledge of the spatial distribution of these tissues derived from probability maps.[47] Gray and white matter segments were extracted to remove nonbrain voxels and then underwent nonlinear normalization to the gray-and-white image template in SPM99 using 7×8×7 basis functions, 12 nonlinear iterations, and medium nonlinear regularization. The resulting images were segmented, producing gray matter, white matter, and cerebrospinal fluid tissue maps in Montreal Neurological Institute (MNI) space having excluded nonbrain voxels. Optimized methods, as described by Good et al,[46] were used to incorporate information from the deformation fields using a modulation step to preserve within-voxel volumes that may have been altered during nonlinear normalization. Voxel values in segmented images were multiplied by Jacobian determinants, derived from spatial normalization, to provide intensity correction for the induced regional volumetric changes. Analysis of modulated data tests for regional differences in absolute tissue volume. Unmodulated data analysis is a complementary test for regional differences in tissue concentration per unit volume based on differences in image intensity.[46-48]

MAGNETIZATION TRANSFER RATIO

Axial images were acquired parallel to the anteroposterior commissural axis. Spatial normalization involved registration of the T2-weighted images, which are implicitly registered (from acquisition) to the MTR images, into standard space. This inherent coregistration of an MTR image and a T2-weighted image allows us to apply registration parameters determined from T2-weighted images (whose contrast matches the MNI template) to MTR images (for which no template is available). The registration used a modified algorithm for 3-dimensional alignment of positron emission tomographic images, relying on anatomic information to align 2 images by calculating the least squares difference of the 2 images on a voxel-by-voxel basis and iteratively moving the images relative to one another to minimize this cost function.[49,50] The T2-weighted images were registered to the MNI T2-weighted average brain in SPM99 using affine 12-parameter, 3-dimensional linear transformations through a 2-stage process. For each participant, a transformation was first found between the T2-weighted image and the MNI T2-weighted average brain, retaining all tissue within the image (brain parenchyma, skull, scalp muscle and fat, and other extracranial tissue). Although reasonably robust, the registration is potentially susceptible to motion artifacts of brain relative to surrounding tissue. To overcome this, the inverse of the transformation found was applied to a version of the MNI T2-weighted average brain from which the skull had been removed. This transformed the skull-stripped MNI template to the native image space of the particular participant, allowing it to be used as a mask to remove nonbrain tissue from the individual participant's T2-weighted image. Each skull-stripped T2-weighted image thus created was then registered to the skull-stripped T2-weighted MNI atlas, transforming it into MNI space. As mask and T2-weighted images have now been skull stripped, this second registration is much more robust. This final transformation was then applied to the participant's MTR image, mapping it into MNI space. Nonbrain features were removed by masking with the skull-stripped T2-weighted MNI average brain. Thus, MTR images were normalized to MNI space but were not subjected to warping or segmentation. Resolution of voxel size of 1×1×5 mm was maintained for MTR images because, unlike SPGR data, resampling 1×1×5-mm MTR images to a 2×2×2-mm isotropic voxel size would have produced only a small increase in signal-to-noise ratio. To determine whether MTR changes were in gray or white matter, we overlaid MTR decreases in patients onto thresholded a priori gray and white matter probability maps provided with SPM99 using the "write filtered" function. A threshold of 16384 (50% of 32768, the intensity representing a probability of 1 in the images) on the white matter map was chosen to identify areas having a greater

than 50% probability of being in white matter rather than gray matter.[38]

SMOOTHING

Taking account of voxel size and the size of structures within which abnormalities were predicted, images were smoothed to 15 mm (MTR) and 12 mm (SPGR) using a full-width–half-maximum Gaussian filter to improve the signal-to-noise ratio, allow for intersubject anatomical variability, and render the data more normally distributed by the central limit theorem. The probability distributions used in SPM99 for voxel and cluster analysis are approximations, which are valid within certain limits, especially with respect to smoothness and number of images. Low smoothing (full-width–half-maximum <3 times voxel size) with low *df* can cause aberrant voxel-level results. Consequently, smoothing of 3 times voxel size is recommended.[51,52] Accordingly, we selected 15-mm full-width–half-maximum smoothing for MTR (3 times voxel size). This relatively high degree of smoothing also helped overcome problems due to the multislice nature of the MTR, which reduced the accuracy of data reconstruction in the slice direction during normalization. For SPGR data, we selected 12-mm full-width–half-maximum smoothing, the spatial scale at which the analysis is most sensitive to differences in regional gray matter. This spatial scale also allows comparison with previous SPM99 voxel-based studies in chronic schizophrenia.[53-55] Each voxel in the smoothed data represents a locally weighted average intensity from a region of surrounding voxels defined by the size of the smoothing kernel.

STATISTICAL ANALYSIS

Group comparisons for MTR (whole brain) and SPGR (both gray matter and white matter maps) between patients with first-episode schizophrenia and controls were performed based on the general linear model and the theory of Gaussian random fields[56] using 2-sample *t* tests to compare populations with 1 scan per participant. Thresholds for MTR and SPGR data were set at 40% of mean image intensity to minimize low signal-to-noise voxels. Only voxels exceeding this intensity threshold (40% of mean image intensity) were included in the analyses. As calculation of mean intensity includes all the (very-low-intensity) pixels outside the head, the cutoff value of 40% of this value should not exclude any pixels that are fully brain tissue. This procedure excluded noise areas outside the brain or in the ventricles. Proportional scaling was used to normalize image intensity in SPGR gray and white matter maps. Using 2 contrasts, the analysis detected whether each voxel had a greater or lesser probability of change, that is, a reduction or increase in the parameter of interest in patients with first-episode schizophrenia compared with controls. The resulting set of voxel values for each contrast constitutes a statistical parametric map of the *t* statistic.

This study was a structural VBM analysis, and, consequently, we selected a study threshold of $t>3.24$ ($P<.001$, uncorrected). Statistical parametric mapping was originally designed to analyze functional data, and correction for multiple comparisons can be considered overly conservative when applied to structural data.[57] We validated our analysis parameters by dividing the control subjects into 2 subgroups matched for age, handedness, and sex. At the threshold of $t>3.24$ ($P<.001$, uncorrected), there were no voxel-level differences in the MTR or SPGR (gray and white matter) between the 2 subgroups of controls, suggesting that this threshold minimizes false positives.

We also report cluster-level statistics for the MTR. Data histograms in a large single-slice region of interest (ROI) incorporating gray and white matter resembled a Gaussian distribution. This satisfies suggested criteria for using cluster size to assess significance in SPM99, considered appropriate only if data are normally distributed.[47] This was not the case for SPGR segmented gray and white matter data. Consequently, we used only voxel-level thresholds for SPGR analysis.

RESULTS

There were no differences for age ($t=0.96$; $P=.34$), sex ($z=0.81$; $P=.42$), handedness ($z=0.46$; $P=.64$), *National Adult Reading Test* premorbid IQ ($t=1.17$; $P=.27$), or paternal social class ($z=0.86$; $P=.39$) between patients with first-episode schizophrenia and controls using *t* tests for continuous variables and Mann-Whitney tests for categorical variables (Table 1).

SPGR GROUP DIFFERENCES

Neither modulated (optimized) nor unmodulated (standard) SPGR T1-weighted gray matter and white matter maps revealed any significant differences between patients and controls for voxel-level statistics at a threshold of $t=3.24$ ($P<.001$, uncorrected). Thus, regional atrophy was not detected because we did not demonstrate any significant regional differences in absolute tissue volume or tissue concentration per unit of volume of gray or white matter in patients with first-episode schizophrenia compared with matched controls.

MTR GROUP DIFFERENCES

At the study statistical threshold of $t>3.24$ ($P<.001$, uncorrected), the MTR was reduced bilaterally in patients with first-episode schizophrenia compared with controls in the insula and adjacent white matter incorporating the fasciculus uncinatus, the right anteromedial frontal lobe extending into the anterior cingulate bilaterally, the right inferior and superior temporal gyrus, the left precuneus, and the left cerebellum (**Figures 1**, **2**, and **3** and **Table 2**). Using the segmented white matter map, we ascertained that the MTR decreases were predominantly cortical, extending into white matter adjacent to the insula, encompassing the fasciculus uncinatus. To exclude the possibility that these were chance findings (type I error), a further analysis was undertaken correcting for multiple comparisons using Gaussian random fields ($t>4.61$; $P<.05$, corrected). Reductions in the MTR in the right medial prefrontal cortex, left insular cortex, and left fasciculus uncinatus survived this correction (Table 2). No MTR increases were observed in patients compared with controls at a threshold of $t>3.24$ ($P<.001$, uncorrected).

We conducted a post hoc validation study to confirm the SPM99 findings using ROI methods in native-space MTR images. Rectangular ROIs (37.9 mm^2) were placed in the medial prefrontal cortex and insula using a standardized protocol in a sample of 8 male, right-handed patients with first-episode schizophrenia and age-, handedness-, and sex-matched controls using DispImage[59] software. Axial proton-density slices were used to identify the lowest slice in which the head of the cau-

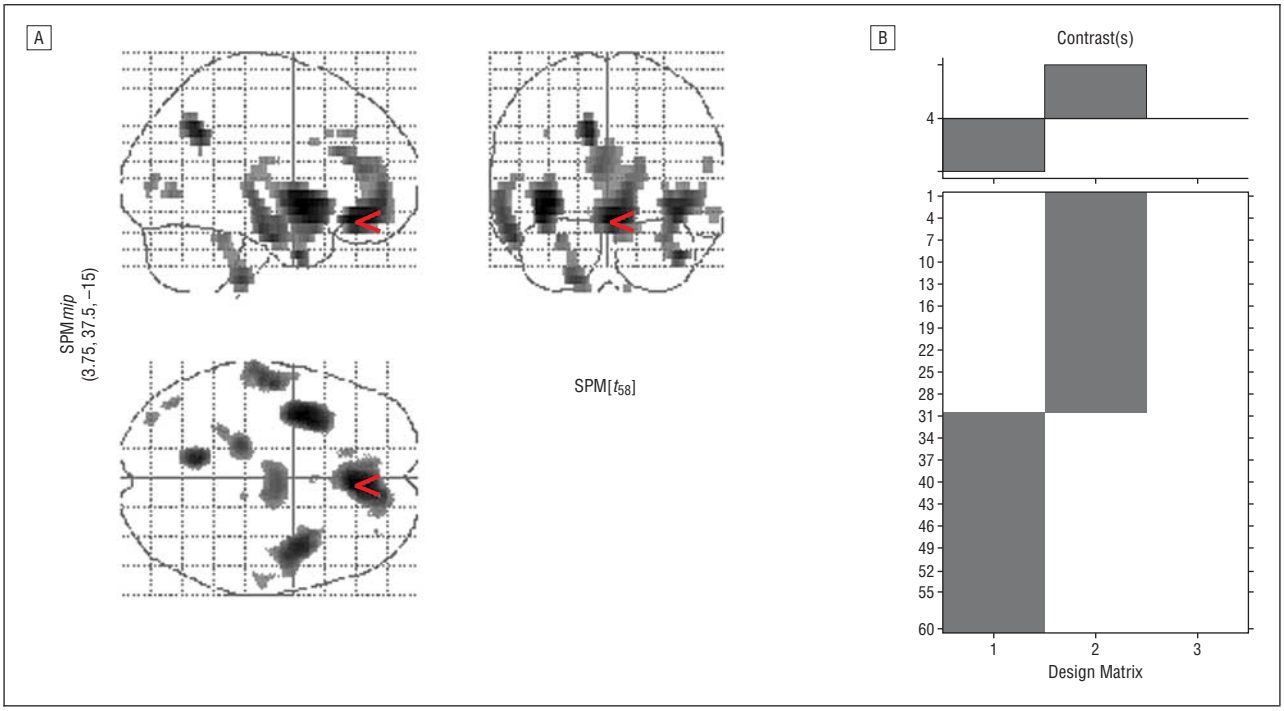

Figure 1. Glass brain image of magnetization transfer ratio reductions in patients with first-episode schizophrenia vs controls. Arrowheads indicate peak voxel. SPM indicates statistical parametric map. Height threshold: t=3.24; P=.001.

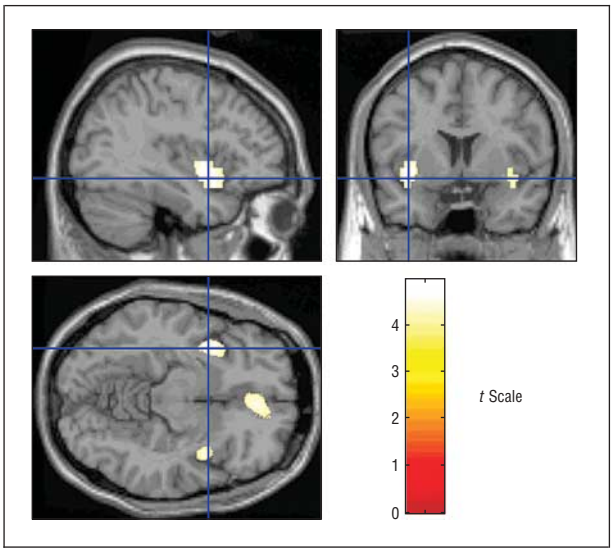

Figure 2. Magnetization transfer ratio reductions in patients with first-episode schizophrenia vs controls (peak voxel in the left insula) demonstrating bilateral reductions in the insula and subcortical white matter rendered onto a T1-weighted image (threshold t=3.97).

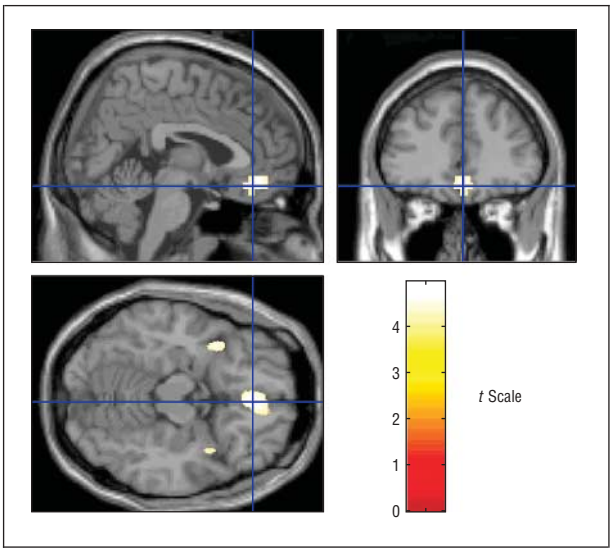

Figure 3. Magnetization transfer ratio reductions in patients with first-episode schizophrenia vs controls (peak voxel in the right prefrontal cortex) demonstrating bilateral (right greater than left) reductions rendered onto a T1-weighted image (threshold t=3.97).

date was visible. Bilateral ROIs were placed in the medial prefrontal cortex, adjacent to the interhemispheric fissure, midway between the frontal pole and the anterior margin of the head of the caudate. Similarly, bilateral ROIs were also placed in the long gyrus of the insula in the adjacent slice. Proton-density images were coregistered to MTR images during acquisition, as previously described. The ROIs were automatically transferred to the coregistered MTR image using DispImage. Care was taken to avoid partial volume effects. The ROIs were placed masked to participant identity. Decreased MTRs were found using Mann-Whitney tests in the right prefrontal cortex and insula (bilaterally) that are consistent with the SPM99 analysis (**Table 3**).

COMMENT

The results of this study suggest that frontotemporal MTR abnormalities involving cortex and white matter are already present at the first episode of schizophrenia. The neuropathological basis for cortical MTR changes remains to be determined, but a variety of abnormalities could cause

Table 2. SPM Statistics of Relative Regional MTR Decreases in 30 Patients* With First-Episode Schizophrenia vs 30 Controls†

Brodmann Area	Anatomical Area	Cluster Level (*P* Value)	Voxel Level (*t*)	Coordinates, mm		
				x	*y*	*z*
A11	Right gyrus rectus (medial pfc)‡		4.96	4	36	–14
A11	Right gyrus rectus (medial pfc)		4.59	8	39	–15
A10	Right gyrus rectus (medial pfc)		4.07	10	50	–7
A32	Left anterior cingulate		3.80	–4	40	12
A24	Left anterior cingulate	.003	3.75	–3	33	17
A9	Right gyrus frontalis medialis		3.75	15	50	6
A24	Left anterior cingulate		3.69	–1	25	22
A32	Right anterior cingulate		3.59	1	37	17
A32	Right anterior cingulate		3.57	2	38	12
	Left insula‡		4.95	–37	6	–9
wm	Left fasciculus uncinatus‡	.03	4.94	–34	8	–5
wm	Left fasciculus uncinatus‡		4.92	–36	4	–5
wm	Left fasciculus uncinatus		4.50	–31	14	–5
	Right insula		4.39	40	4	–9
A20	Right inferior temporal gyrus		4.21	41	1	–30
	Right insula		4.17	44	–1	–4
wm	Right fasciculus uncinatus		4.16	36	8	–5
wm	Right fasciculus uncinatus	.02	3.65	32	7	–21
A22	Right superior temporal gyrus		3.62	52	–3	–1
wm	Right fasciculus uncinatus		3.57	33	14	–5
	Right insula		3.50	40	–10	0
	Right insula		3.30	43	–13	5
A7	Left precuneus	.32	4.08	–12	–57	40
A21	Left middle temporal gyrus	.11	4.14	–54	–12	–25
A21	Left middle temporal gyrus		4.06	–58	–18	–20
	Left cerebellum	.26	4.00	–28	–43	–25
	Left cerebellum		3.68	–24	–40	–25
A37	Left inferior temporal gyrus	.79	3.59	–42	–71	0
A37	Left inferior temporal gyrus		3.29	–41	–74	5

Abbreviations: MNI, Montreal Neurological Institute; MTR, magnetization transfer ratio; pfc, prefrontal cortex; SPM, statistical parametric mapping; wm, white matter.

*Twenty-nine patients with first-episode schizophrenia and 1 with schizophreniform psychosis.

†Coordinates have been converted from MNI space to Talairach space using transformations (available at http://www.mrc-cbu.cam.ac.uk/Imaging/mnispace.html) to allow Talairach anatomical localization.[58]

‡Regions surviving thresholding for multiple comparisons over the whole brain using Gaussian random fields (t_{58} = 4.61; P = .05).

MTR reductions by decreasing the bound proton pool. Although creatine, choline, and *N*-acetylaspartate–related compounds are thought to contribute, the specific molecules responsible for the MTI signal in gray matter are yet to be specified. However, the MTI signal depends on macromolecular density, that is, mainly cell membrane proteins and phospholipids in gray matter and myelin in white matter. Reductions in the MTR in gray matter are likely to be related to decreased cell number, cell size, or dendritic density or may reflect abnormal cell membrane structure. White matter MTR reductions are likely to be related to abnormalities in myelin or reduced axonal density.

The anteromedial prefrontal cortex in schizophrenia has received little attention, although results of animal studies[60] suggest that it may be relevant. Voxel-based studies in chronic schizophrenia have demonstrated anteromedial prefrontal cortex gray matter reductions in some[55,61,62] but not all[54] of a small number of studies. Region of interest studies have been complicated by methodological differences, with few studies evaluating frontal lobe subregions. In a study[63] of patients with chronic schizophrenia and neocortex segmented into 48 topographic regions, the greatest volumetric reductions were in medial and orbitoprefrontal cortices, anterior cingulate gyrus, paracingulate gyrus, and insula. Anterior prefrontal cortex has been associated with monitoring of self-generated information and selection of appropriate executive processes, playing a central role in mediating dorsolateral and ventrolateral prefrontal cortical interaction.[64] Impairment in anteromedial prefrontal regions may contribute to some of the cognitive deficits in schizophrenia.

The anterior cingulate may be relevant to several psychiatric disorders having connections with the hippocampus, orbitofrontal cortex, and amygdala. In schizophrenia, abnormalities in the anterior cingulate include increased glutamatergic axons,[65] axospinous synapses,[66] decreased inhibitory interneurons,[67] and projection neuron loss in deeper laminae.[68] Anterior cingulate volume reductions have been reported in first-episode[16] and chronic[61,63] schizophrenia. Functional imaging data suggest that anterior cingulate cortex may be essential for the internal monitoring necessary to engage top-down attentional processes in adapting to a changing environment.[69,70] Disruption of cingulate-striate circuits has

Table 3. Post hoc Region of Interest Analysis of MTRs in the Prefrontal Cortex and Insula in a Sample of 8 Male, Right-handed Patients With First-Episode Schizophrenia and 8 Matched Control Subjects Using Native-Space MTR Images*

Variable	First-Episode Schizophrenia, Mean ± SD	Control Subjects, Mean ± SD	Mann-Whitney Test
Age, mean ± SD (range), y	26.9 ± 8.5 (18-45)	28.7 ± 3.2 (25-34)	$U = 19.0$ $z = -1.34$ $P = .17$
Left prefrontal cortex MTR	32.8 ± 0.84	33.5 ± 0.75	$U = 20.0$ $z = -1.26$ $P = .21$
Right prefrontal cortex	32.1 ± 0.60	33.5 ± 0.83	$U = 4.5$ $z = -2.89$ $P = .004$†
Left insula MTR	31.6 ± 0.55	32.7 ± 0.44	$U = 2.0$ $z = -3.16$ $P = .002$†
Right insula MTR	31.8 ± 1.01	32.8 ± 0.99	$U = 9.5$ $z = -2.36$ $P = .02$†

Abbreviation: MTR, magnetization transfer ratio.
*Data are given as mean ± SD. Rectangular regions of interest (37.9 mm^2) were placed in the medial prefrontal cortex and long gyrus of the insula using a standardized protocol.
†Regions with significant MTR reductions using Mann-Whitney tests.

been associated with apathy and a lack of drive,[71] characteristic negative symptoms of schizophrenia.

Recent studies have found decreased insular volume in first-episode[16] and chronic[54,61] schizophrenia. Functional imaging studies[72,73] have reported reduced cerebral blood flow in insular cortex during verbal fluency and recognition memory tasks. The insula may also have a pivotal role in cognitive and emotional processes, permitting the internal representation of external events,[74,75] and in the differentiation of internally and externally generated sensory stimuli.[76] Impairment of these processes may mediate some perceptual disturbances in schizophrenia.

Abnormalities in the fasciculus uncinatus replicate findings from a recent study[61] of patients with schizophrenia and predominantly negative symptoms. The fasciculus uncinatus is a bundle of association fibers connecting orbitofrontal, superofrontal, and middle frontal gyri with anterior temporal lobe cortex, and it may play an important role in schizophrenia. It contains the lateral cholinergic pathway originating in the nucleus basalis of Meynert and innervates frontal, parietal, and temporal neocortex.[77] Cortical cholinergic pathways are important mediators in processing information essential for cognition.[78] Fasciculus uncinatus abnormalities may explain the reduced postsynaptic prefrontal muscarinic receptor binding recently reported in schizophrenia.[79] Right frontotemporal disconnection after injury to the right ventral frontal lobe and underlying fasciculus uncinatus leads to impaired awareness of self over time, which is integral to the formulation and implementation of future goals.[80]

White matter abnormalities may be relevant in schizophrenia. Schizophrenialike symptoms occur in metachromatic leukodystrophy,[81] and recent diffusion imaging studies have reported reduced anisotropy in prefrontal white matter[82,83] and corpus callosum,[84] suggesting myelin or axonal abnormalities. Differential expression of myelination-related genes in dorsolateral prefrontal cortex,[85] apoptosis, and necrosis of oligodendroglial cells and damaged myelin sheaths in prefrontal cortex and caudate nucleus have been reported in schizophrenia.[86] Myelination of frontotemporal connections continues into early adulthood.[87] Delayed or abnormal frontotemporal myelination in schizophrenia could explain the onset of symptoms in early adulthood.

We did not demonstrate atrophy. Our volumetric findings are contrary to those of some studies demonstrating decreases in medial temporal lobe structures, particularly the hippocampus,[17,88,89] superior temporal gyrus,[90] insula,[16] and prefrontal cortex[54] in first-episode schizophrenia. This may reflect the heterogeneity of first-episode schizophrenia populations, which include patients with variable disease outcomes. However, there is considerable variance in image intensity in small medial temporal lobe structures, and some subcortical gray matter structures have image intensities similar to white matter, increasing risk of tissue misclassification during segmentation in these regions. Partial volume effects may have contributed, as the model assumes that all voxels contain only 1 tissue type, and those containing more than 1 may be modeled incorrectly. Accordingly, ROI methods may be more sensitive in such subcortical structures. These methodological problems, however, are unlikely to account for our findings for several reasons. First, the normalization and segmentation procedures used in SPM99 have been considered robust and accurate for volumetric T1-weighted images.[47] Second, gray matter losses have been reported in cortical and subcortical gray matter in patients with chronic schizophrenia and other conditions using similar analysis methods.[38,55,91-93] Third, we excluded nonbrain voxels and used a modulation step that allows comparison of absolute amounts of gray matter. Finally, despite normal findings in volumetric im-

aging, MTR abnormalities were detected in regions where volumetric deficits have been reported in chronic and first-episode studies.

The discrepancy between circumscribed MTR abnormalities in first-episode schizophrenia reported herein and the more widespread abnormalities previously reported in chronic schizophrenia by Foong et al[38] deserve comment. There are 2 possible explanations. The first assumes that any brain abnormalities in schizophrenia are static and that widespread cortical abnormalities occur only in those with severe, chronic disease. If this model is correct, a much larger sample of patients with first-episode schizophrenia than is reported herein would be required to ensure that sufficient numbers of patients destined to have severe chronic illness were included. The alternative is that brain abnormalities are progressive, at least in some patients, and that cortical abnormalities spread as disease becomes chronic. Support for this explanation accrues from the longitudinal study of Thompson et al[94] reporting progressive gray matter loss extending from parietal regions to include temporal, dorsolateral prefrontal, and frontal eyefield cortices in a small sample with childhood-onset schizophrenia. Longitudinal studies are ongoing to determine whether the abnormalities we reported are progressive and the relationship to illness course and treatment response.

Several limitations of this study should be mentioned. There are potential limitations in the use of VBM that have been discussed in detail elsewhere.[46-48,95] Data on MTRs could be prone to partial volume effects due to the 5-mm slices. However, we did not segment or warp the MTR data, which minimizes the risk of tissue misclassification. In addition, our post hoc native-space MTR ROI analysis was consistent with the SPM99 analysis. We reported cluster and voxel analyses for MTR data. Histograms of our data samples incorporating gray and white matter on a given slice resembled a Gaussian distribution, as previously demonstrated in chronic schizophrenia in reporting cluster analysis.[38] The use of cluster size to assess significance in SPM is appropriate only if the data are normally distributed.[47] It is possible that the MTR signal may not be normally distributed locally. A permutation analysis may be more reliable for cluster analysis in future studies. Most patients were receiving neuroleptic agents, and it could be argued that our findings may be different in a drug-naive population. However, there is little evidence from neuropathological studies, conducted mainly in animals, to suggest that neuroleptic medication causes or exacerbates brain abnormalities in schizophrenia,[7] and most of our patients were receiving atypical neuroleptic agents for short periods, making this even less likely. Nonetheless, the effects of neuroleptic medication use on MTRs have not been studied and could be a potential confound. We repeated our analysis excluding the 5 unmedicated patients. Decreases in MTRs were found in the same regions. We did not analyze unmedicated patients separately because the sample size would have insufficient *df* to produce meaningful results. Our sample was relatively small, and it may not be possible to generalize our findings to other first-episode schizophrenia populations.

Submitted for publication April 2, 2002; final revision received February 6, 2003; accepted February 7, 2003.

This study was supported by a grant from the Wellcome Trust, London.

We thank the members of the NMR Research Unit, Institute of Neurology, University College London, for their assistance, and we thank all the patients and volunteers who participated in the study.

Corresponding author and reprints: Manny S. Bagary, MRCPsych, Box 15, Section of Neuropsychiatry and NMR Research Unit, Institute of Neurology, University College London, Queen Square, London, WC1N 3BG England (e-mail: m.bagary@ion.ucl.ac.uk).

REFERENCES

1. Shenton ME, Dickey CC, Frumin M, McCarley RW. A review of MRI findings in schizophrenia. *Schizophr Res.* 2001;49:1-52.
2. Wright IC, Rabe-Hesketh S, Woodruff PWR, David AS, Murray RM, Bullmore ET. Meta-analysis of regional brain volumes in schizophrenia. *Am J Psychiatry.* 2000; 157:16-25.
3. Wright IC, Sharma T, Ellison ZR, McGuire PK, Friston KJ, Brammer MJ, Murray RM, Bullmore ET. Supra-regional brain systems and the neuropathology of schizophrenia. *Cereb Cortex.* 1999;9:366-378.
4. Robbins T. The case for fronto-striatal dysfunction in schizophrenia. *Schizophr Bull.* 1990;16:391-401.
5. Buchsbaum MS, Haier RJ, Potkin SG, Nuechterlein K, Bracha HS, Katz M, Lohr J, Wu J, Lottenberg S, Jerabek PA. Frontostriatal disorder of cerebral metabolism in never-medicated schizophrenics. *Arch Gen Psychiatry.* 1992;49:935-942.
6. Friston KJ, Frith CD. Schizophrenia: a disconnection syndrome? *Clin Neurosci.* 1995;3:89-97.
7. Harrison P. The neuropathology of schizophrenia: a critical review of the data and their interpretation. *Brain.* 1999;122(pt 4):593-624.
8. Andreason NC, Arndt S, Swayze V, Cizado T, Flaum M, O'Leary D, Ehardt JC, Yuh WT. Thalamic abnormalities in schizophrenia visualized through magnetic resonance image averaging. *Science.* 1994;266:294-298.
9. Puri BK, Hutton SB, Saeed N, Oatridge A, Hajnal JV, Duncan L, Chapman MJ, Barnes TR, Bydder GM, Joyce EM. A serial longitudinal quantitative MRI study of cerebral changes in first-episode schizophrenia using image segmentation and subvoxel registration. *Psychiatry Res.* 2001;106:141-150.
10. DeLisi LE, Tew W, Xie S, Hoff AL, Sakuma M, Kushner M, Lee G, Shedlack K, Smith AM, Grimson R. A prospective follow-up study of brain morphology and cognition in first episode schizophrenic patients: preliminary findings. *Biol Psychiatry.* 1995;38:349-360.
11. Lim KO, Tew W, Kushner M, Chow K, Matsumoto B, DeLisi LE. Cortical gray matter volume deficit in patients with first-episode schizophrenia. *Am J Psychiatry.* 1996;153:1548-1553.
12. Zipursky RB, Lambe EK, Kapur SK, Mikulis DJ. Cerebral gray matter volume deficits in first-episode psychosis. *Arch Gen Psychiatry.* 1998;55:540-546.
13. Lieberman JA, Jody D, Alvir JM, Ashtari M, Levy DL, Bogerts B, Degreef G, Mayerhoff DI, Cooper T. Brain morphology, dopamine, and eye-tracking abnormalities in first-episode schizophrenia: prevalence and clinical correlates. *Arch Gen Psychiatry.* 1993;50:357-368.
14. Barr WB, Ashtari M, Bilder M, Degreef G, Lieberman J. Brain morphometric comparison of first-episode schizophrenia and temporal lobe epilepsy. *Br J Psychiatry.* 1997;170:515-519.
15. Gur RE, Turetsky BI, Cowell PE, Finkelman C, Maany V, Grossman RI, Arnold SE, Bilker WB, Gur RC. Temporolimbic volume reductions in schizophrenia. *Arch Gen Psychiatry.* 2000;57:769-775.
16. Crespo-Facorro B, Kim J, Andreasen NC, O'Leary DS, Bockholt HJ, Magnotta V. Insular cortex abnormalities in schizophrenia: a structural magnetic resonance imaging study of first-episode patients. *Schizophr Res.* 2000;46:35-43.
17. Heckers S. Neuroimaging studies of the hippocampus in schizophrenia. *Hippocampus.* 2001;11:520-528.
18. DeLisi LE, Stritzke P, Riordan H, Holan V, Boccio A, Kushner M, McClelland J, Van Eyl O, Anand A. The timing of brain morphological changes in schizophrenia and their relationship to clinical outcome. *Biol Psychiatry.* 1992;31:241-254.
19. Bilder RM, Wu H, Bogerts B, Degreef G, Ashtari M, Alvir JM, Snyder PJ, Lieberman JA. Absence of regional hemispheric volume asymmetries in first-episode schizophrenia. *Am J Psychiatry.* 1994;151:1437-1447.
20. Razi K, Greene KP, Sakuma M, Ge S, Kushner M, DeLisi LE. Reduction of the parahippocampal gyrus and the hippocampus in patients with chronic schizophrenia. *Br J Psychiatry.* 1999;174:512-519.

21. Laakso MP, Tiihonen J, Syvalahti E, Vilkman H, Laakso A, Alakare B, Rakkolainen V, Salokangas RK, Koivisto E, Hietala J. A morphometric MRI study of the hippocampus in first-episode, neuroleptic-naive schizophrenia. *Schizophr Res.* 2001;50:3-7.
22. Wolff SD, Balaban RS. Magnetization transfer contrast (MTC) and tissue water proton relaxation in vivo. *Magn Reson Med.* 1989;10:135-144.
23. Henkelman RM, Stanisz GJ, Graham SJ. Magnetization transfer in MRI: a review. *NMR Biomed.* 2001;14:57-64.
24. Meyerhoff DJ. Proton magnetization transfer of metabolites in human brain. *Magn Reson Med.* 1999;42:417-420.
25. Mottershead JP, Thornton JS, Clemence M, Scaravilli F, Newcombe J, Cuzner ML, Barker GJ, Tofts PS, Parker GJM, Ordidge RJ, Miller DH, McDonald WI. Correlation of spinal cord axonal density with post mortem NMR measurements in multiple sclerosis and controls [abstract]. *Proc Int Soc Magn Reson Med.* 1998; 6:T2163.
26. van Waesberghe, Kamphorst W, De Groot CJ, van Walderveen MA, Castelijns JA, Ravid R, Lycklama a Nijeholt GJ, van der Valk P, Polman CH, Thompson AJ, Barkhof F. Axonal loss in multiple sclerosis lesions: magnetic resonance imaging insights into substrates of disability. *Ann Neurol.* 1999;46:747-754.
27. Dousset V, Grossman RI, Ramer KN, Schnall MD, Young LH, Gonzalez-Scarano F, Lavi E, Cohen JA. Experimental allergic encephalomyelitis and multiple sclerosis: lesion characterization with magnetization transfer imaging. *Radiology.* 1992;182:483-491.
28. Deloire-Grassin MS, Brochet B, Quesson B, Delalande C, Dousset V, Canioni P, Petry KG. In vivo evaluation of remyelination in rat brain by magnetization transfer imaging. *J Neurol Sci.* 2000;178:10-16.
29. Lexa FJ, Grossman RI, Rosenquist AC. MR of wallerian degeneration in the feline visual system: characterization by magnetization transfer rate with histopathologic correlation. *AJNR Am J Neuroradiol.* 1994;15:201-212.
30. Kimura H, Meaney DF, McGowan JC, Grossman RI, Lenkinski RE, Ross DT, McIntosh TK, Gennarelli TA, Smith DH. Magnetization transfer imaging of diffuse axonal injury following experimental brain injury in the pig: characterization by magnetization transfer ratio with histopathologic correlation. *J Comput Assist Tomogr.* 1996;20:540-546.
31. Gass A, Barker GJ, Kidd D, Thorpe JW, MacManus D, Brennan A, Tofts PS, Thompson AJ, McDonald WI, Miller DH. Correlation of magnetization transfer ratio and clinical disability in multiple sclerosis. *Ann Neurol.* 1994;36:62-67.
32. Silver NC, Barker GJ, MacManus DC, Thorpe JW, Howard R, Miller DH. Decreased magnetization transfer ratio due to demyelination: a case of central pontine myelinolysis. *J Neurol Neurosurg Psychiatry.* 1996;61:208-209.
33. Kado H, Kimura H, Tsuchida T, Yonekura Y, Tokime T, Tokuriki Y, Itoh H. Abnormal magnetization transfer ratios in normal-appearing white matter on conventional MR images of patients with occlusive cerebrovascular disease. *AJNR Am J Neuroradiol.* 2001;22:922-927.
34. Bosma GP, Rood MJ, Zwinderman AH, Huizinga TW, van Buchem MA. Evidence of central nervous system damage in patients with neuropsychiatric systemic lupus erythematosus, demonstrated by magnetization transfer imaging. *Arthritis Rheum.* 2000;43:48-54.
35. Ernst T, Chang L, Witt M, Walot I, Aronow H, Leonido-Yee M, Singer E. Progressive multifocal leukoencephalopathy and human immunodeficiency virus–associated white matter lesions in AIDS: magnetization transfer MR imaging. *Radiology.* 1999;210:539-543.
36. Sinson G, Bagley LJ, Cecil KM, Torchia M, McGowan JC, Lenkinski RE, McIntosh TK, Grossman RI. Magnetization transfer imaging and proton MR spectroscopy in the evaluation of axonal injury: correlation with clinical outcome after traumatic brain injury. *AJNR Am J Neuroradiol.* 2001;22:143-151.
37. Cercignani M, Bozzali M, Iannucci G, Comi G, Filippi M. Magnetization transfer ratio and mean diffusivity of normal appearing white and gray matter from patients with multiple sclerosis. *J Neurol Neurosurg Psychiatry.* 2001;70:311-317.
38. Foong J, Symms MR, Barker GJ, Maier M, Woermann FG, Miller DH, Ron MA. Neuropathological abnormalities in schizophrenia: evidence from magnetization transfer imaging. *Brain.* 2001;124:882-892.
39. Selemon LD, Goldman-Rakic PS. The reduced neuropil hypothesis: a circuit based model of schizophrenia. *Biol Psychiatry.* 1999;45:17-25.
40. Andreason N. Methods for assessing positive and negative symptoms in schizophrenia: positive and negative symptoms and syndromes. In: Andreason N, ed. *Modern Problems in Pharmacopsychiatry.* Vol 24. Basel, Switzerland: S Karger AG; 1990:73-85.
41. Asberg M, Montgomery SA, Perris C, Schalling D, Sedvall G. A comprehensive psychopathological rating scale. *Acta Psychiatr Scand Suppl.* 1978;271:5-27.
42. Annett MA. A classification of hand preference by association analysis. *Br J Psychol.* 1970;61:303-321.
43. Goldthorpe JH, Hope K. *The Social Grading of Occupations: A New Approach and Scale.* Oxford, England: Clarendon Press; 1974.
44. Nelson H, Willison J. *The National Adult Reading Test (NART).* 2nd ed. Windsor, England: NFER-Nelson; 1991.
45. Barker GJ, Tofts PS, Gass A. An interleaved sequence for accurate and reproducible clinical measurement of magnetization transfer ratio. *Magn Reson Imaging.* 1996;14:403-411.
46. Good CD, Johnsrude IS, Ashburner J, Henson RN, Friston KJ, Frackowiak RS. A voxel-based morphometric study of ageing in 465 normal adult human brains. *Neuroimage.* 2001;14(pt 1):21-36.
47. Ashburner J, Friston KJ. Voxel based morphometry: the methods. *Neuroimage.* 2000;11:805-821.
48. Ashburner J, Friston KJ. Why voxel-based morphometry should be used. *Neuroimage.* 2001;14:1238-1243.
49. Symms M, Barker G, Holmes A. A rapid automated system for detection of serial changes in transient ischaemic attack using registration and subtraction of three dimensional images [abstract]. *Proc Int Soc Magn Reons Med.* 1997;5: 584.
50. Woods R, Cherry S, Mazziotta J. Rapid automated algorithm for aligning and reslicing PET images. *J Comput Assist Tomogr.* 1992;16:620-633.
51. Friston KJ, Holmes A, Poline JB, Price CJ, Frith CD. Detecting activations in PET and fMRI: levels of inference and power. *Neuroimage.* 1996;4(pt 1):223-235.
52. Stoeckael J, Poline JB, Malandain G, Ayache N, Darcourt J. Smoothness and degrees of freedom restrictions when using SPM99 [abstract]. *Hum Brain Mapp.* 2001;14(suppl):11365.
53. Wright IC, McGuire PK, Poline JB, Travere JM, Murray RM, Frith CD, Frackowiak RS, Friston KJ. A voxel-based method for the statistical analysis of gray and white matter density applied to schizophrenia. *Neuroimage.* 1995;2:244-252.
54. Wright IC, Ellison ZR, Sharma T, Friston KJ, Murray RM, McGuire PK. Mapping of gray matter changes in schizophrenia. *Schizophr Res.* 1999;35:1-14.
55. Wilke M, Kaufmann C, Grabner A, Putz B, Wetter TC, Auer DP. Gray matter changes and correlates of disease severity in schizophrenia: a statistical parametric mapping study. *Neuroimage.* 2001;13:814-824.
56. Poline JB, Worsley KJ, Evans AC, Friston KJ. Combining spatial extent and peak intensity to test for activations in functional imaging. *Neuroimage.* 1997;5:83-96.
57. Sowell ER, Thompson PM, Holmes CJ, Batth R, Jernigan TL, Toga AW. Localizing age-related changes in brain structure between childhood and adolescence using statistical parametric mapping. *Neuroimage.* 1999;9(pt 1):587-597.
58. Talairach J, Tournoux P. *Co-planar Stereotaxic Atlas of the Human Brain.* New York, NY: Thieme Medical Publisher; 1988.
59. Plummer DL. DispImage: a display and analysis tool for medical images. *Riv Neuroradiol.* 1992;5:489-495.
60. Yee BK. Cytotoxic lesion of the medial prefrontal cortex abolishes the partial reinforcement extinction effect, attenuates prepulse inhibition of the acoustic startle reflex and induces transient hyperlocomotion, while sparing spontaneous object recognition memory in the rat. *Neuroscience.* 2000;95:675-689.
61. Sigmundsson T, Suckling J, Maier M, Williams S, Bullmore E, Greenwood K, Fukuda R, Ron M, Toone B. Structural abnormalities in frontal, temporal and limbic regions and interconnecting white matter tracts in schizophrenic patients with prominent negative symptoms. *Am J Psychiatry.* 2001;158:234-243.
62. Hulshoff Pol HE, Schnack HG, Mandl RC, van Haren NE, Koning H, Collins DL, Evans AC, Kahn RS. Focal gray matter density changes in schizophrenia. *Arch Gen Psychiatry.* 2001;58:1118-1125.
63. Goldstein JM, Goodman JM, Seidman LJ, Kennedy DN, Makris N, Lee H, Tourville I, Caviness VS, Faraone SV, Tsuang MT. Cortical abnormalities in schizophrenia identified by structural magnetic resonance imaging. *Arch Gen Psychiatry.* 1999;56:537-547.
64. Fletcher PC, Henson RN. Frontal lobes and human memory: insights from functional neuroimaging. *Brain.* 2001;124(pt 5):849-881.
65. Benes FM, Vincent SL, Alsterberg G, Bird ED, SanGiovanni JP. Increased GABAA receptor binding in superficial layers of cingulate cortex in schizophrenics. *J Neurosci.* 1992;12:924-929.
66. Aganova EA, Uranova NA. Morphometric analysis of synaptic contacts in the anterior limbic cortex in the endogenous psychoses. *Neurosci Behav Physiol.* 1992; 22:59-65.
67. Benes FM, McSparren J, Bird ED, SanGiovanni JP, Vincent SL. Deficits in small interneurons in prefrontal and cingulate cortices of schizophrenic and schizoaffective patients. *Arch Gen Psychiatry.* 1991;48:996-1001.
68. Benes FM, Vincent SL, Todtenkopf M. The density of pyramidal and nonpyramidal neurons in anterior cingulate cortex of schizophrenic and bipolar subjects. *Biol Psychiatry.* 2001;50:395-406.
69. Bunge SA, Ochsner KN, Desmond JE, Glover GH, Gabrieli JD. Prefrontal regions involved in keeping information in and out of mind. *Brain.* 2001;124:2074-2086.
70. van Veen V, Cohen JD, Botvinick MM, Stenger VA, Carter CS. Anterior cingulate cortex, conflict monitoring, and levels of processing. *Neuroimage.* 2001;14: 1302-1308.
71. Cummings JL. Frontal-subcortical circuits and human behaviour. *Arch Neurol.* 1993;50:873-878.

72. Curtis VA, Bullmore ET, Brammer MI, Wrigth IC, Williams SC, Morris RG, Sharma TS, Murray RM, McGuire PK. Attenuated frontal activation during verbal fluency tasks in patients with schizophrenia. *Am J Psychiatry.* 1998;155:1056-1063.
73. Crespo-Facorro B, Wiser AK, Andreasen NC, O'Leary DS, Watkins GL, Ponto LL, Hichwa RD. Neural basis of novel and well-learned recognition memory in schizophrenia: a positron emission tomography study. *Hum Brain Mapp.* 2001;12:219-231.
74. Augustine JR. Circuitry and functional aspects of the insular lobe in primates including humans. *Brain Res Brain Res Rev.* 1996;22:229-244.
75. Cancelliere AE, Kertesz A. Lesion localisation in acquired deficits of emotional expression and comprehension. *Brain Cogn.* 1990;13:133-147.
76. Mesulam M, Mufson E. Insula of the Old World monkey, II: efferent cortical output and comments on function. *J Comp Neurol.* 1982;212:38-52.
77. Selden NR, Gitelman DR, Salamon-Murayama N, Parrish TB, Mesulam MM. Trajectories of cholinergic pathways within the cerebral hemispheres of the human brain. *Brain.* 1998;121(pt 12):2249-2257.
78. Mesulam MM. Behavioral neuroanatomy of cholinergic innervation in the primate cerebral cortex. *EXS.* 1989;57:1-11.
79. Crook JM, Tomaskovic-Crook E, Copolov DL, Dean B. Low muscarinic receptor binding in prefrontal cortex from subjects with schizophrenia: a study of Brodmann's areas 8, 9, 10, and 46 and the effects of neuroleptic drug treatment. *Am J Psychiatry.* 2001;158:918-925.
80. Levine B, Black SE, Cabeza R, Sinden M, Mcintosh AR, Toth JP, Tulving E, Stuss DT. Episodic memory and the self in a case of isolated retrograde amnesia. *Brain.* 1998;121(pt 10):1951-1973.
81. Hyde TM, Ziegler JC, Weinberger DR. Psychiatric disturbances in metachromatic leukodystrophy: insights into the neurobiology of psychosis. *Arch Neurol.* 1992;49:401-406.
82. Buchsbaum MS, Tang CY, Peled S, Gudbjartsson H, Lu D, Hazlett EA, Downhill J, Haznedar M, Fallon JH, Atlas SW. MRI white matter diffusion anisotropy and PET metabolic rate in schizophrenia. *Neuroreport.* 1998;9:425-430.
83. Lim KO, Hedehus M, Moseley M, de Crespigny A, Sullivan E, Pfeferbaum A. Compromised white matter tract integrity in schizophrenia inferred from diffusion tensor imaging. *Arch Gen Psychiatry.* 1999;56:367-374.
84. Foong J, Maier M, Dark A, Barker GJ, Miller DH, Ron MA. Neuropathological abnormalities of the corpus callosum in schizophrenia: a diffusion tensor imaging study. *J Neurol Neurosurg Psychiatry.* 2000;68:242-244.
85. Hakak Y, Walker JR, Li C, Wong WH, Davis KL, Buxbaum JD, Haroutunian V, Fienberg AA. Genome-wide expression analysis reveals dysregulation of myelination-related genes in chronic schizophrenia. *Proc Natl Acad Sci U S A.* 2001; 98:4746-4751.
86. Uranova N, Orlovskaya D, Vikhreva O, Zimina I, Kolomeets N, Vostrikov V, Rachmanova V. Electron microscopy of oligodendroglia in severe mental illness. *Brain Res Bull.* 2001;55:597-561.
87. Benes FM. Myelination of cortical-hippocampal relays during late adolescence. *Schizophr Bull.* 1989;15:585-593.
88. Bilder RM, Bogerts B, Ashtari M, Wu H, Alvir JM, Jody D, Reiter G, Bell L, Lieberman JA. Anterior hippocampal volume reductions predict frontal lobe dysfunction in first episode schizophrenia. *Schizophr Res.* 1995;17:47-58.
89. Copolov D, Velakoulis D, McGorry P, Carina Mallard, Yung A, Rees S, Jackson G, Rehn A, Brewer W, Pantelis C. Neurobiological findings in early phase schizophrenia. *Brain Res Brain Res Rev.* 2000;31:157-165.
90. Hirayasu Y, Shenton ME, Salisbury DF, Dickey CC, Fischer IA, Mazzoni P, Kisler T, Arakaki H, Kwon JS, Anderson JE, Yurgelun-Todd D, Tohen M, McCarley RW. Lower left temporal lobe MRI volumes in patients with first-episode schizophrenia compared with psychotic patients with first-episode affective disorder and normal subjects. *Am J Psychiatry.* 1998;155:1384-1391.
91. Rosen HJ, Gorno-Tempini ML, Goldman WP, Perry RJ, Schuff N, Weiner M, Feiwell R, Kramer JH, Miller BL. Patterns of brain atrophy in frontotemporal dementia and semantic dementia. *Neurology.* 2002;58:198-208.
92. Ananth H, Popescu I, Critchley HD, Good CD, Frackowiak RS, Dolan RJ. Cortical and subcortical gray matter abnormalities in schizophrenia determined through structural magnetic resonance imaging with optimized volumetric voxel-based morphometry. *Am J Psychiatry.* 2002;159:1497-1505.
93. Thieben MJ, Duggins AJ, Good CD, Gomes L, Mahant N, Richards F, McCusker E, Frackowiak RS. The distribution of structural neuropathology in pre-clinical Huntington's disease. *Brain.* 2002;125(pt 8):1815-1828.
94. Thompson PM, Vidal C, Giedd JN, Gochman P, Blumenthal J, Nicolson R, Toga AW, Rapoport JL. Mapping adolescent brain change reveals dynamic wave of accelerated gray matter loss in very early-onset schizophrenia. *Proc Natl Acad Sci U S A.* 2001;98:11650-11655.
95. Bookstein FL. Voxel-based morphometry should not be used with imperfectly registered images. *Neuroimage.* 2001;14:1454-1462.